Ceramics-Silikáty 68 (2), 205-215 (2024)
www.ceramics-silikaty.cz doi: 10.13168/cs.2024.0020

PROPERTIES OF CEMENT COMPOSITES CONTAINING QUATERNISED POLY(4-VINYLPYRIDINE) GRAFTED GRAPHENE OXIDE

#LITING QIN, ZIWEI YIN

School of Resources Engineering, Heilongjiang University of Technology, Jixi, 158100, P. R. China

#E-mail: 15020140213@xs.hnit.edu.cn

Submitted December 06, 2023; accepted March 11, 2024

Keywords: Cement-based composite, Graphene oxide, Quaternised poly(4-vinylpyridine), Mechanical properties

The agglomeration of graphene oxide (GO) in cement mortar poses a serious obstacle to the development of the mechanical properties of cement composites and limits its practical application. To address this issue, quaternised poly(4-vinylpyridine) grafted GO (QP4VP@GO) were prepared through chemical grafting of quaternised P4VP onto the surface of GO using atomic transfer radical polymerisation (ATRP) and the QP4VP@GO doped cement-based composites (QP4VP@GO/C) were subsequently prepared. X-ray diffraction (XRD), scanning electron microscopy (SEM), and Fourier transform infrared spectroscopy (FT-IR) were utilised to investigate the structural characteristics of the modified GO. It was observed that the dispersion of quaternised-P4VP grafted GO in the calcium hydroxide (Ca(OH)2) solution exhibited better performance compared to GO. Additionally, when 0.03 wt. % of the QP4VP@GO was incorporated into the cement composite, the maximum flexural strength at 28 d of the cement-based composites reached 8.0 MPa, which shows an obvious improvement compared to ordinary Portland cement and GO cement-based composites. Similarly, with the addition of 0.05 wt. % of QP4VP@GO, the maximum compressive strength at 28 d of the cement-based composites was enhanced to 72.4 MPa. Furthermore, the SEM characterisation results demonstrated that the inclusion of QP4VP@GO facilitated the enhancement of cement hydration, impeded the crack expansion, and improved the mechanical properties of the cement composites.

INTRODUCTION

Cement-based materials are commonly employed in the construction of building structures due to their notable benefits such as easy sampling, high compressive strength, better durability and strong plasticity [1]. However, it is important to acknowledge their inherent drawbacks, including insufficient early strength, poor crack resistance, low tension or flexural strength, high brittleness and slow setting and hardening, which often contribute to the expansion and cracking of weakened interface areas, particularly in fine pores and micro-cracks, making it challenging to meet the increasingly stringent requirements of the construction industry for concrete performance [2-4]. Improving the flexural strength of cement-based materials was challenging on its own, with the most effective approach being the incorporation of reinforced materials. While using traditional microfibres as reinforcement materials can enhance the crack resistance and toughness of cement-based composites to a certain degree, its influence on improving the microstructure of cement-based materials itself remains limited [5, 6]. In particular, the effectiveness of these fibres in addressing nanoscale harmful pores is minimal. Therefore, it is necessary to develop new technologies or high-performance materials to eliminate the above-mentioned disadvantages of cement-based materials.

Carbon nanomaterials have gained considerable attention in cement-based materials due to their numerous advantages, including high aspect ratio, large specific surface area, nanoscale particle size and the ability to regulate the structure of cement hydrates at the nanoscale and profoundly impact its mechanical properties, thus mitigating the formation of nanoscale cracks and enhancing the toughness of the concrete [7-9]. Among various carbon nanomaterials, graphene oxide (GO) has emerged as a promising enhancer for cement-based materials due to its high specific surface area, unique layered structure, and the presence of oxygen-containing functional groups (improvement of hydrophilicity) attached to its edges and surfaces [10-13]. During the process of cement hydration, the hydroxyl, epoxy, and carboxyl groups of GO chemically react with the cement hydrates, resulting in the accelerated hydration and densification of the cement matrix [14-16]. Consequently, the blend of cement and GO is strengthened, resulting in the enhanced load-bearing capacity, crack resistance and flexural strength of cement-based composites.

While the addition of GO significantly enhances the properties of cement-based materials, achieving the proper dispersibility of GO in cement remains a challenging task. Park et al. revealed that the oxygenated functional groups on GO nanosheets can bind to Mg^{2+} and Ca^{2+}, forming products that reduce its dispersibility by reducing the hydrophilic functional groups [17]. However, considering the abundance of Ca^{2+} in the cement mortar, the dispersibility of GO is likely to be compromised. Therefore, it is crucial to investigate the dispersion ability of GO and explore methods to enhance its dispersibility, as the effective dispersion of nanomaterials in the cement is directly linked to their ability to improve the mechanical and other relevant properties.

Currently, numerous research studies have endeavoured to address the issue of GO agglomeration within cement [9, 10]. In one such study, Duan et al. employed silica fume to mechanically separate GO flakes, impeding their tendency to aggregate in cement. As a result, the dispersibility of GO within the cement mortar improved significantly [18]. Similarly, Guo et al. discovered that a polycarboxylate (PC) superplasticiser can effectively interact with GO even in an alkaline environment [19]. Notably, the dispersion effect achieved by the PC surpassed that of other dispersants and exhibited remarkable stability. Nevertheless, the integration of a secondary material in intricate cement systems can introduce numerous uncertainties and uncontrollable variables, resulting in new interface complications that are detrimental to improving the mechanical properties and preventing cracks in cement-based materials. Thus, implementing *in situ* modifications on the surface of GO can provide an effective solution to the aforementioned challenges [20-23]. Very recently, Pan et al. developed a straightforward method to modify PC with GO, not only affording excellent dispersion of PC+GO in the alkali environment of cement, but also improving the mechanical properties of cement composites [24].

Keeping this in mind, the present study sets sights on the captivating N-alkylated quaternised poly(4-vinylpyridine) (QP4VP) onto the surface of GO by atom transfer radical polymerisation (ATRP) [25-27], which birthed a mesmerising entity known as the QP4VP@GO complex (Figure 1). The introduction of hydrophilic Q4PVP onto the GO surface can improve the hydrophilicity of GO and its dispersibility in cement, thereby improving the performance of cement-based materials. The goal was to elevate the dispersion ability of GO within the cement mortar, a feat achieved with the aid of this captivating complex. Specifically, the obtained QP4VP@GO complex was incorporated into the cement matrix to study the effect of QP4VP@GO on the mechanical properties and durability of the cement composites. The dispersion mechanism of P4VP@GO was also revealed.

EXPERIMENTAL

Materials

The graphite powder, concentrated hydrochloric acid (37 wt. %), calcium hydroxide, concentrated sulfuric acid (98 wt. %), potassium permanganate, sodium nitrate, hydrogen peroxide (30 wt. %), triethanolamine, polycarboxylate superplasticizer, N-(2-aminoethyl)-2-bromo-2-methylpropanamide·HCl, dimethylformamide (DMF), 4VP, cuprous bromide (CuBr) and pentamethyldiethylenetriamine (PMDETA) were purchased from Aladdin Co., Ltd and used as received. The cement was ordinary Portland cement (P. O42.5 refers to GB 175–2007, Foshan Runhe Building Materials Co., Ltd.) and the chemical compositions of that are summarised in Table 1. The water used to mix cement mortar was ordinary tap water.

Table 1. Chemical compositions of the cement.

Sample	Weight percentage of each composition (%)						
	CaO	SiO_2	Al_2O_3	MgO	Fe_2O_3	SO_3	K_2O
Cement	60.56	23.04	6.03	1.42	4.52	0.38	0.70

Preparation of GO

GO was prepared through a series of steps according to the Hummers' method [28]. Firstly, 6.0 g of graphite powder, 9.0 g of sodium nitrate, and 180 mL of concentrated sulfuric acid were added to a flask. To ensure a controlled reaction, the flask was placed in an ice-water bath at 5 °C and the mixture was pre-stirred for even distribution. While maintaining the temperature at 5 °C, 30.0 g of potassium permanganate was slowly added to the flask while stirring for another 120 minutes. Then, the reaction was stirred for an additional 3 h at 35 °C by slowly adding 400 mL of deionised water. Next, the temperature was raised to 95 °C and the reaction was maintained for 10 minutes. At this stage, 300 mL of deionised water and 36 mL of hydrogen peroxide were added, and the stirring continued until the solution no longer had bubbles and turned brown. Once the solution reached this point, it was filtered while hot and then thoroughly washed with diluted hydrochloric acid (5 wt. %) and deionised water. Subsequently, freeze-drying was carried out to obtain the final product.

Preparation of quaternised-P4VP grafted GO (QP4VP@GO)

To synthesise the GO-initiator, the following process was implemented: initially, a GO suspension was diluted with ultrapure water to a concentration of 4 $mg \cdot mL^{-1}$ and then subjected to ultrasonication for a duration of 30 minutes. Subsequently, 60 mL of the GO solution was combined with 180 mg of the initiator, and the pH of the resulting mixture was adjusted to a range between 9

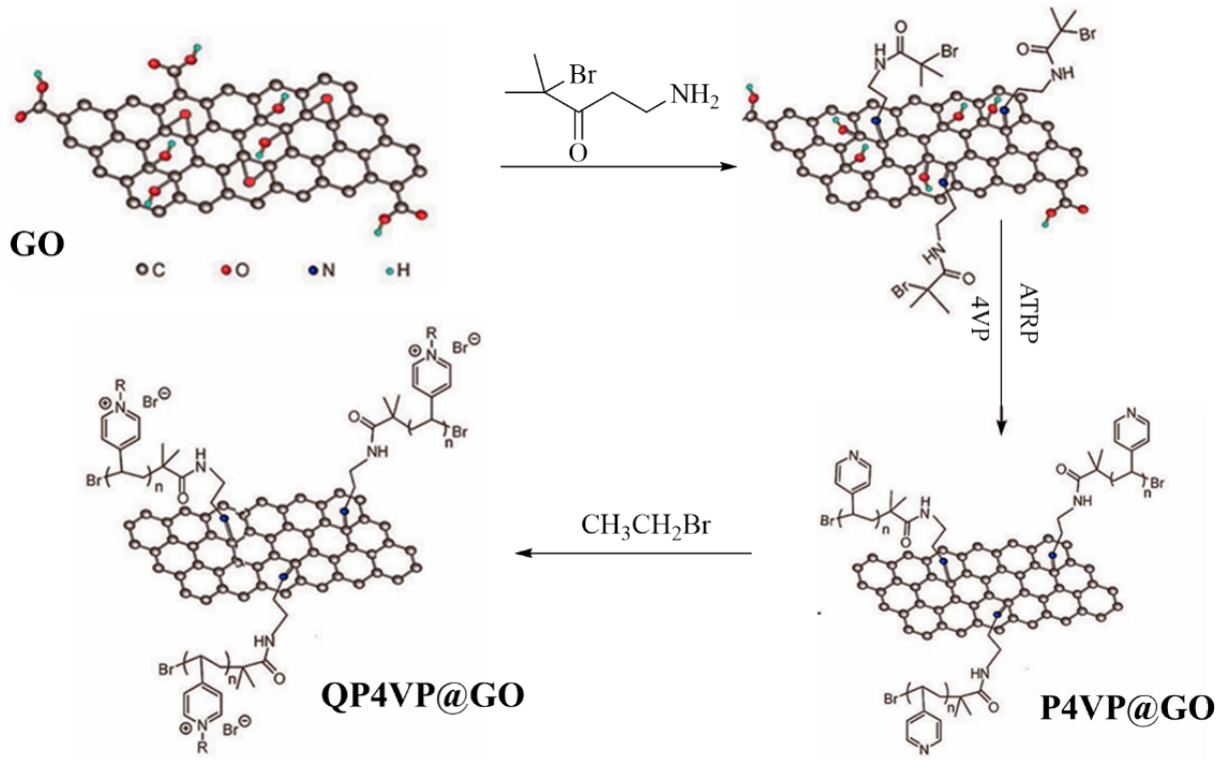

Figure 1. Schematic illustration for the preparation of quaternised P4VP grafted GO (QP4VP@GO).

and 10. After an additional 30 minutes of ultrasonication, the solution was deoxygenated by purging it with nitrogen for 30 minutes. Maintaining a nitrogen atmosphere, the solution was heated at 90 °C for a period of 24 hours, during which the pH was continuously monitored and adjusted to uphold its original state. The resultant solid material was thoroughly washed using ethanol and water in repetitive cycles, followed by re-dispersion in DMF. Centrifugation and ultrasonication were subsequently applied, and the resulting supernatant was retained for further use.

To prepare the P4VP grafted GO (P4VP@GO), the following process was implemented: 5 mL of the GO-initiator solution was combined with a precise quantity of 4VP, and the resulting mixture was purged with nitrogen for a duration of 30 minutes. Subsequently, under a nitrogen atmosphere, CuBr (14.4 mg) and PMDETA (25.0 mg) were introduced. The reaction was allowed to proceed at a temperature of 80 °C for a period of 30 h. Following the reaction, the resulting solid material was thoroughly washed with methanol in repetitive cycles, and then dissolved in DMF.

To prepare the quanternised-P4VP grated GO (QP4VP@GO), the following process was implemented: the obtained P4VP@GO composite was combined with 1-bromoethane and subjected to heating at a temperature of 40 °C for a duration of 2 d, resulting in the formation of QP4VP@GO. Following this, the materials underwent a recovery process, involving thorough washing with methanol for three cycles, followed by re-dissolution in water. The concentration of all the products was determined by calculating the dry weight achieved through freeze drying.

Dispersion test of GO and QP4VP@GO

To simulate the hydration environment of the cement slurry, a 20.0 mmol·L^{-1} solution of calcium hydroxide $Ca(OH)_2$ was prepared. GO and QP4VP@GO were accurately weighed and added to the $Ca(OH)_2$ solution, ensuring a mass concentration of 2.0 mg·mL^{-1} for both components. The solution was then subjected to sonication for 1 h, followed by continuous shaking for 12 h to attain a state of equilibrium.

Preparation of GO and cement composite

Using the cement mass as the basis, varying concentrations of GO, namely 0.01 %, 0.03 % and 0.05 % of its mass, along with quanternised-QP4VP@GO and 0.2 wt. % water reducer, were sequentially measured. Prior to mixing, tap water was added and stirred thoroughly in advance with a water-to-cement mass ratio of 30/100. The aforementioned substances were then poured into a clean cement mortar mixer, where fast and slow stirring speeds were set for 3 and 5 min, respectively. Following the stirring process, the mixed mortar was poured into a mould measuring 50 mm × 50 mm × 250 mm and left to cure in a cement standard curing box for 24 h. After demoulding, the curing process was continued for 3, 7 and 28 days. The resulting cement-based composites, namely the Control (without GO or modified GO), GO/C and QP4VPGO/C, were utilised to test their flexural strength and compressive strength.

Characterisations

An optical microscope (SAGA, SG-300, China) and scanning electron microscope (Hitachi S4300, Japan) were used to observe the dispersity of GO and QP4VP@GO in the $Ca(OH)_2$ solution. The cross-sectional and top view of QP4VP@GO and GO films, and the surface of the cement composites were also characterised by SEM. The zeta potential was performed with Zetasizer Ultra (Mal-vern, U. K.) at 25 °C at a pH of 7.0. Fourier transform infrared (FT-IR) spectra were carried out on a Thermo Fisher Nicolet iS5 FT-IR spectrometer with a potassium bromide (KBr) pellet. An X-ray diffractometer (XRD, Aeris, Malvern, U.K.) was used to investigate the structure of the graphite powder and QP4VP@GO. The mechanical performance of the cement composites, including the flexural strength and compressive strength, was assessed following the guidelines of the Chinese standard (GB/T 17671-1999). Three specimens were tested using a universal testing machine (Instron 5882, USA), and both the mean values and standard deviations were calculated to ensure an accurate evaluation.

RESULTS AND DISCUSSIONS

Structure and morphology characterisation of GO and QP4VP@GO

In Figure 2, the XRD spectra of the original graphite powder and synthesised QP4VP@GO are presented. The spectrum of the graphite powder shows a distinct diffraction characteristic peak at 2θ of 26.6°, which corresponds to the graphite (002) crystal plane and possesses a crystal plane spacing of 0.33 nm. Interestingly, the XRD spectrum of QP4VP@GO does not exhibit the (002) and (004) crystal planes found in graphite. Instead, a novel diffraction characteristic peak emerges at 2θ of 11.4°, demonstrating a low peak intensity. Through crystallographic calculations, the crystal plane spacing of this new peak is determined to be 0.77 nm, in consistent agreement with prior literature reports [29, 30]. This finding signifies the successful synthesis of GO.

The prepared dispersions of QP4VP@GO offer a convenient and practical solution for various applications as they easily form macroscopic, flexible, and free-standing films. The microscopic analysis of the film's cross-section reveals a distinctive layered structure (Figure 3). Unlike the vague lamination observed in GO alone, the incorporation of attached polymer brushes in QP4VP@GO fills the gaps between layers, establishing a continuous network within the composite. Consequently, the cross-section of QP4VP@GO exhibits exceptional packing, resulting in smoother surfaces. The presence of numerous oxygen-containing functional groups in GO causes its edges to curl and adopt an undulating gauze-like shape [31, 32]. Furthermore, the dispersion of quaternised polymer brushes functionalised GO displays superior homogeneity compared

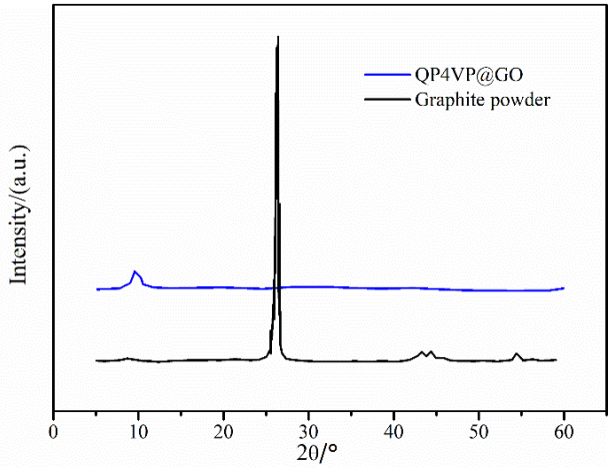

Figure 2. XRD patterns of the graphite powder (blank) and QP4VP@GO (blue).

to GO alone, ensuring a more uniform paper structure upon solvent evaporation. This consistent structure serves as evidence for the successful grafting of QP4VP onto GO.

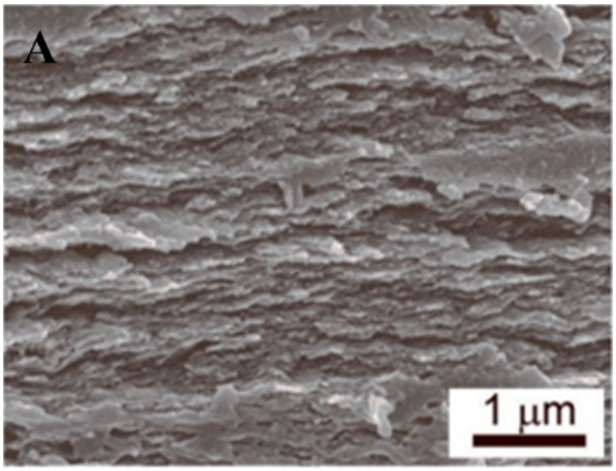

a) cross-sectional SEM images of QP4VP@GO

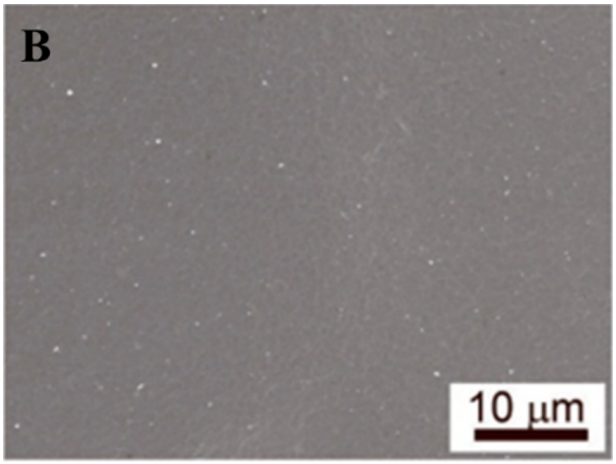

b) top view SEM images of QP4VP@GO

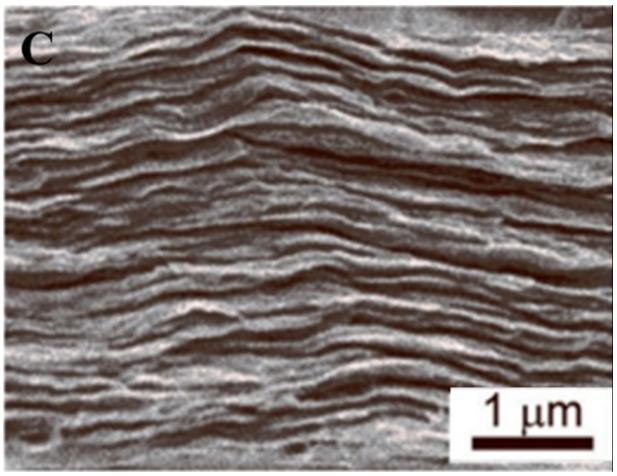

c) cross-sectional SEM images of GO

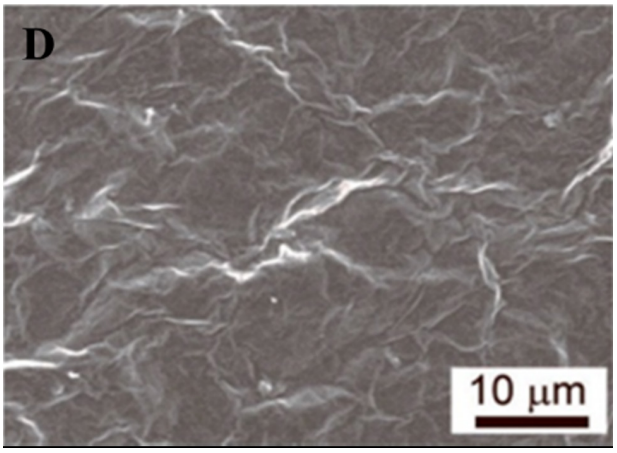

d) top view SEM images of GO

Figure 3. Cross-sectional and top view SEM images of QP4VP@GO and GO.

An FT-IR analysis was conducted to confirm the successful grafting of quaternised P4VP onto GO, as depicted in Figure 4. The FT-IR spectrum of P4VP@GO (blank) revealed characteristic bands at 3428 cm^{-1}, originating from O-H stretching, and at 1718 cm^{-1}, arising from C=O stretching vibrations. Additionally, the presence of a peak at 1600 cm^{-1} indicated the presence of pyridine vibrations from the polymer brushes. Distinctive bands observed at 2920 cm^{-1} and 2845 cm^{-1} can be attributed to the C-H groups of polymerised alkyl chains, whereas the peak at 3018 cm^{-1} could be assigned to the C-H vibrations of the pyridine ring. These particular bands are unique to functionalised GO and are absent in GO alone. The presence of these peaks confirms the successful polymerisation of 4VP on the surface of GO. Furthermore, the disappearance of the signal at 3210 cm^{-1} in QP4VP@GO suggests the quaternisation of pyridine nitrogen atoms by alkyl chains. This quaternisation reaction also caused a shift in the peak position from 1600 cm^{-1} to approximately 1628 cm^{-1}, indicating the C=N stretching vibrations of the pyridine ring. Hence, it can be concluded that additional quaternisation groups were attached to the polymer chains on the surface of GO. In summary, the FT-IR analysis demonstrated the successful grafting of quaternised P4VP onto GO, resulting in the formation of QP4VP@GO, while still large amounts of hydroxyl groups are still present.

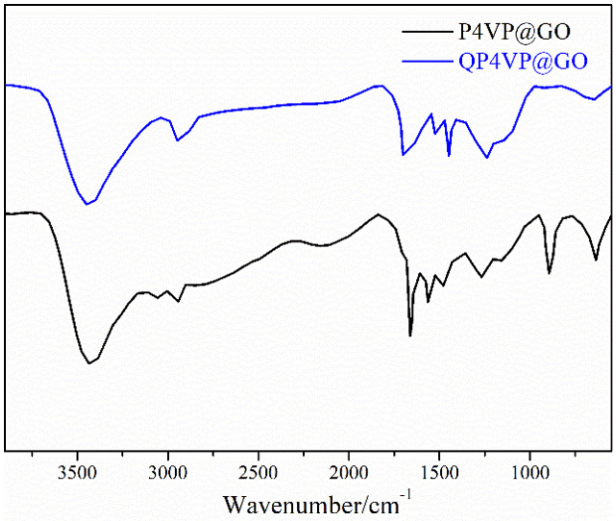

Figure 4. FT-IR spectra of P4VP@GO (blank) and QP4VP@GO (blue).

The dispersion analysis of GO and QP4VP@GO

To mimic the alkaline conditions in cement composites, a solution of $Ca(OH)_2$ was utilised, and the dispersion behaviour of the synthesised GO and QP4VP@GO in this solution was investigated. The relative agglomeration states of GO and QP4VP@GO were examined using optical microscopy and SEM, as illustrated in Figure 5. Figure 4A&B high-light the varying degrees of accumulation of GO and QP4VP-GO in the $Ca(OH)_2$ solution. Notably, QP4VP@GO exhibited significantly weaker aggregation compared to GO. While GO displayed good dispersion in the solution, a study by Park et al. indicated that re-agglomeration of GO occurred due to the stacking and bridging between the GO sheets in the presence of sufficient concentrations of Ca^{2+} ions. In contrast, the modification of GO with QP4VP mitigated its agglomeration behaviour. The presence of grafted cationic P4VP on GO may have a dual effect. Firstly, it enhances the hydrophilicity of GO, making it more water-friendly. Secondly, the electrostatic repulsion (zeta potential is about 30.2 ± 1.3 mV), arising from the presence of cationic grafted chains, hampers the aggregation tendency of GO [33].

Figure 5c depicts the relatively large size of the GO particles, with calcium carbonate ($CaCO_3$) crystals deposited on their surfaces, suggesting the GO

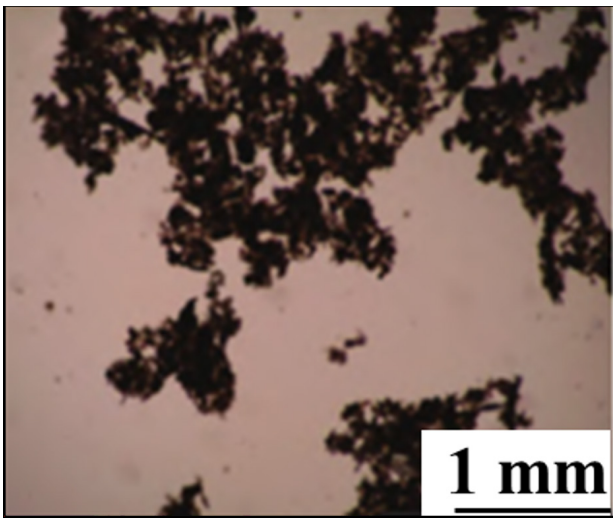

a) optical image of GO

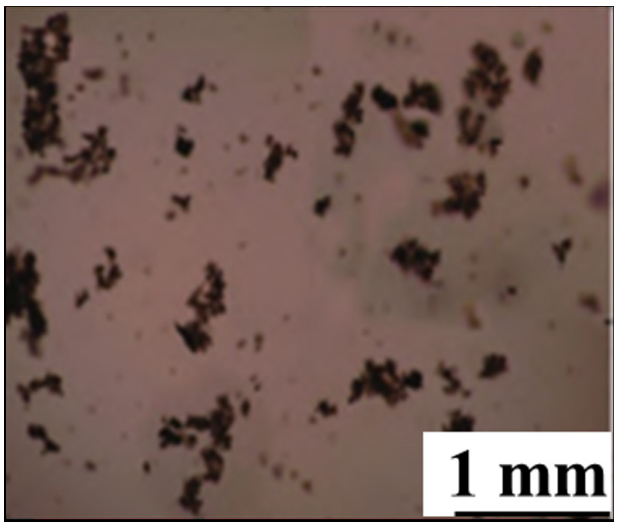

b) optical image of QP4VP@GO

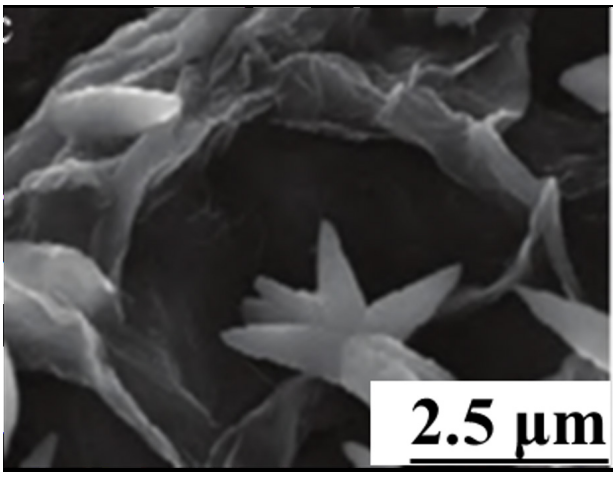

c) SEM image of GO

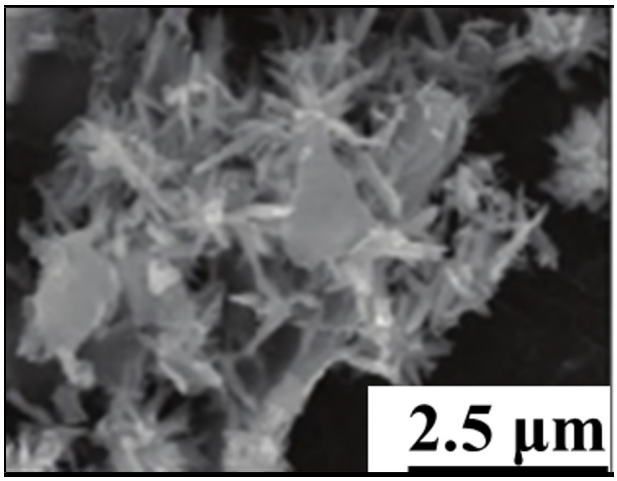

d) SEM image of QP4VP@GO

Figure 5. Optical images and SEM images of GO and QP4VP@GO.

surface underwent chemical cross-linking with Ca^{2+} [17]. In contrast, Figure 5d demonstrates that QP4VP@GO possessed smaller particle sizes, with Ca^{2+} primarily deposited at the edges of the QP4VP@GO sheets. Although quaternised P4VP has been successfully grafted onto GO, there remains a considerable number of functional groups, such as hydroxyl groups, on the surface of the modified GO. However, the presence of these functional groups is significantly reduced compared to un-grafted GO. Consequently, the surface of QP4VP@GO still retains some CaCO3 crystals, albeit in a much lower quantity compared to crystals deposited on GO, which is consistent with the results from FT-IR analysis. QP4VP@GO demonstrated reduced agglomeration compared to GO, with Ca^{2+} ions preferentially depositing at the edges of QP4VP@GO sheets due to the increased presence of hydroxyl groups. These findings provide insights into the interaction between the modified GO in the alkaline environment, which is beneficial for the study of cement composites with additives.

Mechanical properties of cement composites with GO and QP4VP@GO

Figure 6 illustrates the compressive strength and flexural strength of various cement samples, including pure conventional Portland cement blanks, cement complexes supplemented with GO and quaternised P4VP-grafted GO at different time intervals (3, 7, and 28 days). From the figure, it becomes evident that the mechanical properties of cement-based composites undergo similar changes when different amounts of GO and QP4VP@GO are added. Specifically, the compressive strength of the composites increases with higher doping levels of GO or QP4VP@GO at different ages. Remarkably, the flexural strength exhibits an initially increasing and then decreasing trend. At a QP4VP@GO content of 0.03 wt. %, the flexural strength of the cement composite at 28 d reaches its maximum value of 8.0 MPa, which is 42.3 % higher than that of the con-ventional Portland cement sample

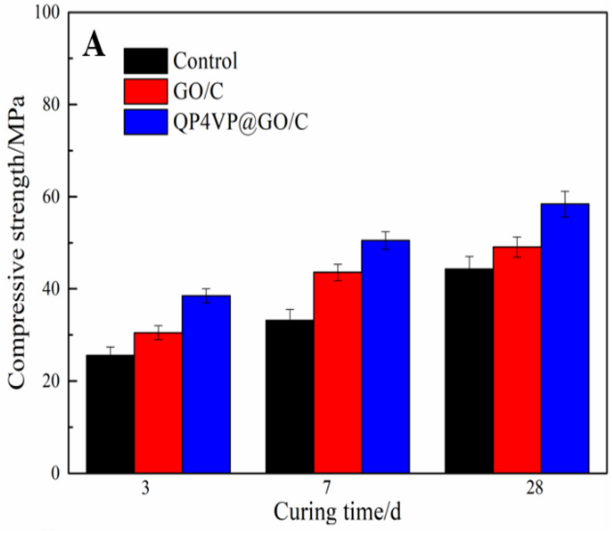

a) 0.01 wt. % GO, 0.01 wt. % QP4VP@GO

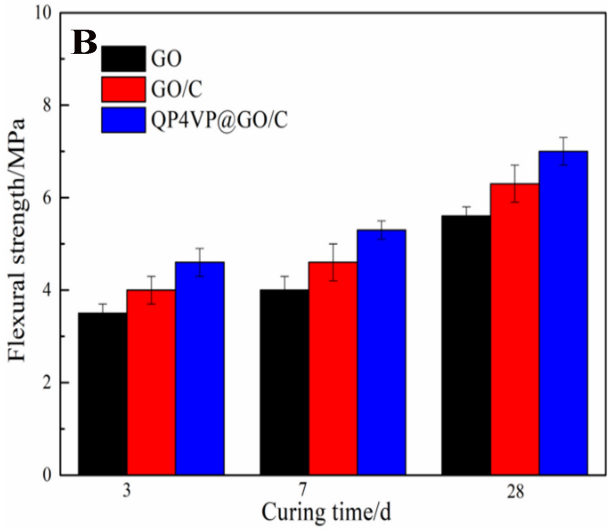

b) 0.01 wt. % GO, 0.01 wt. % QP4VP@GO

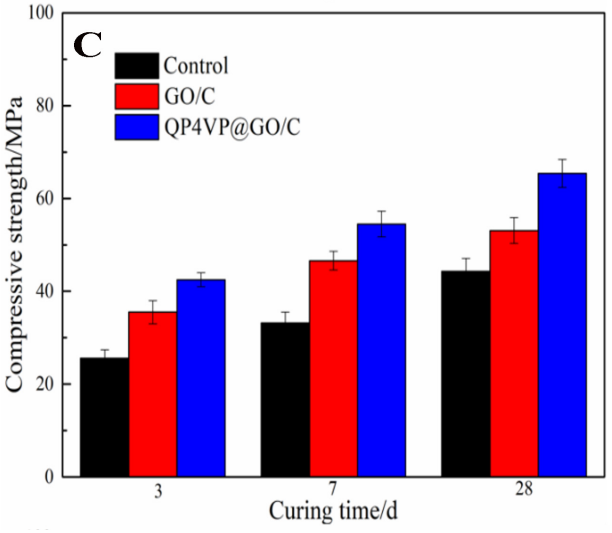

c) 0.03 wt. % GO, 0.03 wt. % QP4VP@GO

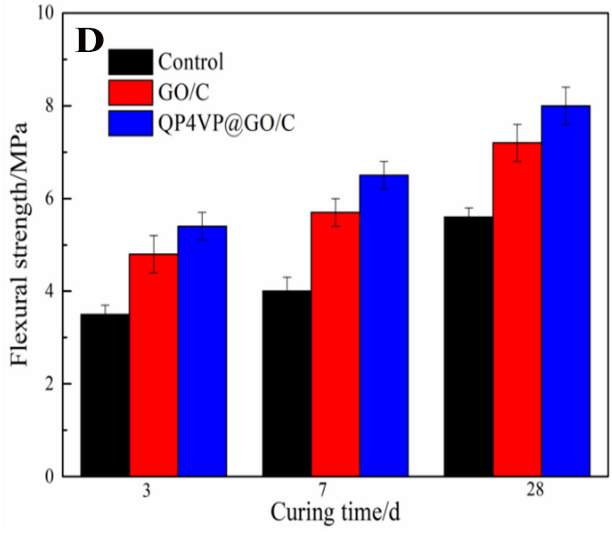

d) 0.03 wt. % GO, 0.03 wt. % QP4VP@GO

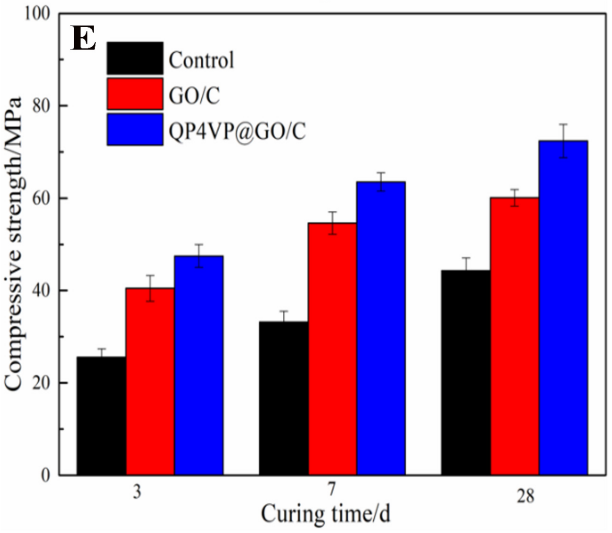

e) 0.05 wt. % GO, 0.05 wt. % QP4VP@GO

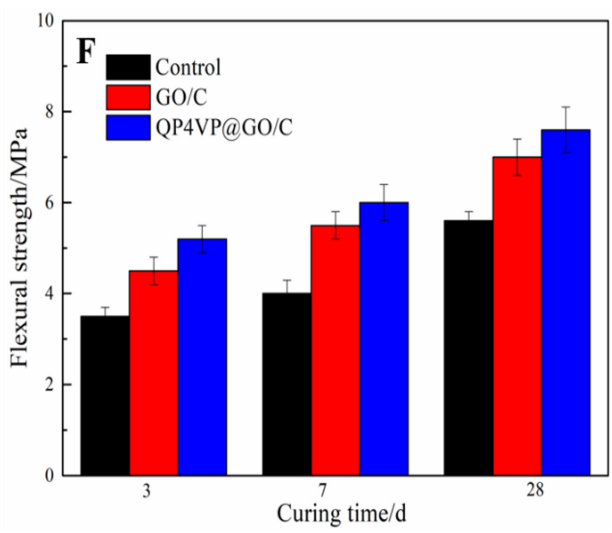

f) 0.05 wt. % GO, 0.05 wt. % QP4VP@GO

Figure 6. The compressive strength of cement composites control and the flexural strength of cement composites control.

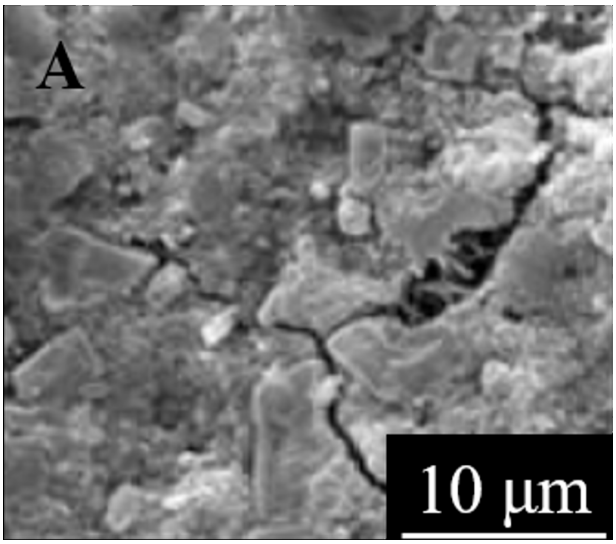

a) ordinary Portland cement

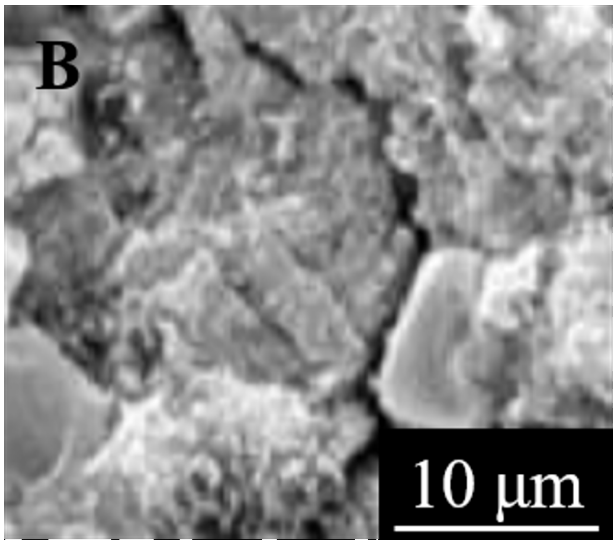

b) ordinary Portland cement

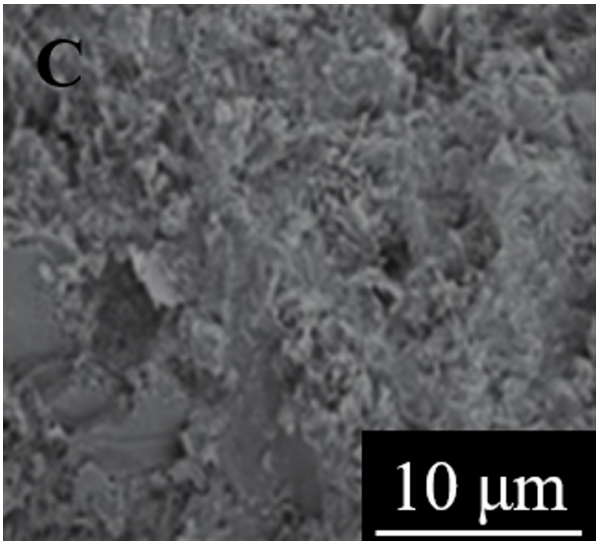

c) doped with GO

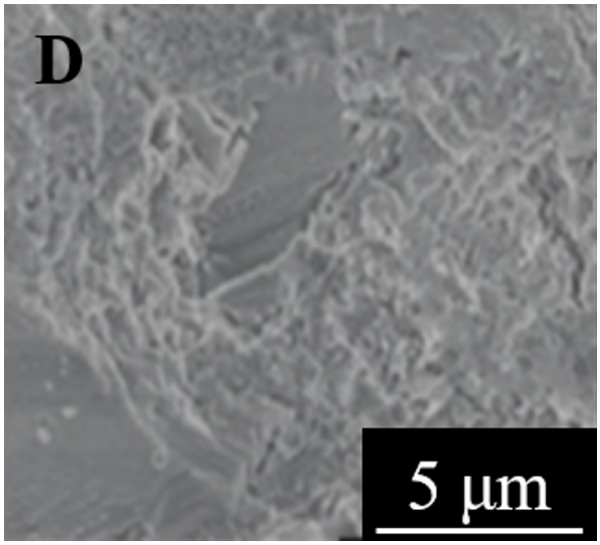

d) doped with GO

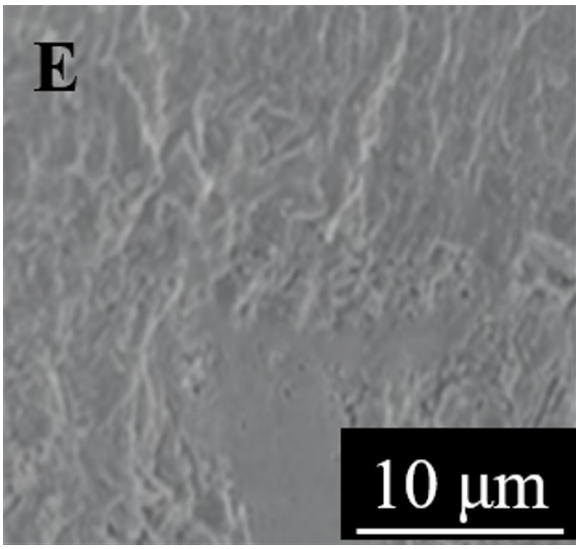

e) doped with QP4VP@GO

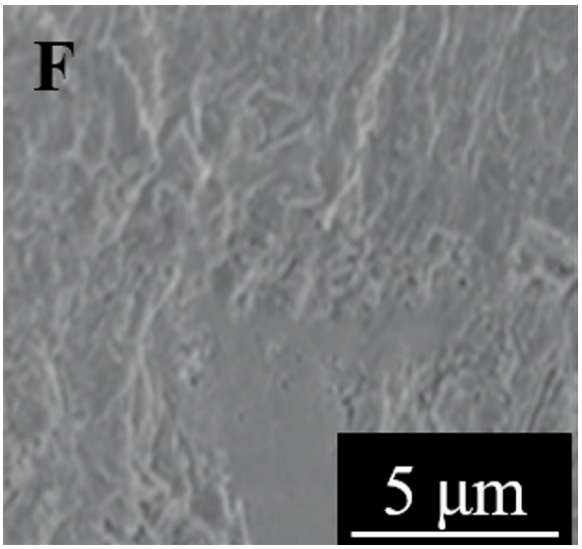

f) doped with QP4VP@GO

Figure 7. SEM images of 28 d hydration products of the cement composites.

and 11.1 % higher than that of cement samples doped with 0.03 wt. % GO. Similarly, at a QP4VP@GO content of 0.05 wt. %, the 28-day compressive strength reaches a maximum of 72.4 MPa, which is 63.1 % higher than that of the Portland cement sample and 16.6 % higher than that of cement samples doped with only 0.05 wt. % GO.

Moreover, when the GO admixture is 0.03 wt. %, the 28-day flexural strength of the GO cement-based composites reaches its peak at 7.2 MPa, which is 28.6 % higher than that of the Portland cement. Furthermore, when the GO additive is 0.05 wt. %, the compressive strength of the GO cement-based composites reaches a maximum of 62.1 MPa at 28 days, which is 40.1 % higher than that of the Portland cement. Based on the experimental results mentioned above, it can be concluded that both GO and QP4VP@GO can enhance the mechanical properties of cement-based composites. Additionally, the use of QP4VP@GO demonstrates a further improvement in the mechanical properties of these composites.

Microstructure of cement composites with GO and QP4VP@GO

Figure 7 depicts the SEM images of the hydration products of ordinary Portland cement, cement-based composites doped with GO, and quaternised polymer-grafted GO (QP4VP@GO) after 28 d. In Figure 7a, it is evident that the ordinary Portland cement's hydrate exhibits numerous cracks, some of which pass through the hydrate. Conversely, Figures 6B&C illustrate that the pores and cracks present in GO cement-based composites are relatively small. Additionally, the cracks appear randomly branched and discontinuous from one another, indicating GO promotes cement hydration and leading to a substantial filling of voids and cracks within the cement matrix [34, 35]. Consequently, this phenomenon contributes to the toughening of the cement composite's mechanical properties. .

For Figures 7d and 7e, it becomes apparent that the cracks in the QP4VP@GO cement-based composites are smaller, and the hydrate crystals display greater maturity, which can be attributed to the effective energy dissipation of GO modified by quaternisation. Such modification benefits from the excellent toughness of QP4VP@GO, enabling it to control nanometre-scale microcracks in the material. As a result, the expansion of cracks is prevented, mitigating material disintegration while simultaneously enhancing its mechanical properties and extending its service life. Therefore, it could be concluded that the introduction of grafted quaternised polymer effectively refines the microstructure of the cement composites.

Figure 8 describes the XRD patterns of the hydration products of the ordinary Portland cement, cement linker, cement-based composites doped with GO, and QP4VP@GO after 28 d. In the XRD patterns, $Ca(OH)_2$ crystals,

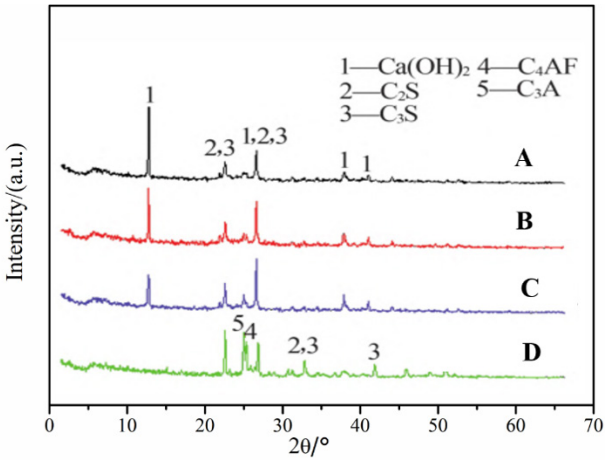

Figure 8. XRD patterns of 28 d hydration products of the cement composites, (A) doped with QP4VP@GO, (B) doped with GO, (C) ordinary Portland cement, (D) cement clinker.

a hydration product, serve as a gauge for the degree of hydration and their diffraction peaks at the 2θ angles of 18.5, 35.4, 48.2, and 51.3° in Figure 8 are typically examined [36,37]. Upon the introduction of GO and QP4VP@GO, the intensity of the $Ca(OH)_2$ peak at 18.5° significantly rose. Notably, cement composites doped with QP4VP@/GO exhibited the highest peak intensity, suggesting their role in fostering cement hydration and bolstering mechanical attributes. The diffraction peaks of tricalcium silicate (C_3S) primarily appeared at the 2θ angles of 30.1, 34.6, and 52.2°, while those of dicalcium silicate (C_2S) were mainly at the 2θ angles of 29.5, 33.8, and 41.7°. This distinction arises from the prevalence of monoclinic, triclinic, and rhomboid crystals in the structures of C_3S and C_2S. Comparatively, cement composites doped with QP4VP@/GO exhibited notably lower peak intensities at the 2θ angles of 30.1, 33.8, 32.0, and 32.5° for tricalcium aluminate (C_3A) and tetracalcium ferric aluminate (C_4AF), indicating QP4VP@/GO's efficacy in enhancing the cement clinker consumption and facilitating full clinker hydration compared to the control and cement composites doped with GO.

CONCLUSIONS

In summary, the successful grafting of quaternised P4VP onto the surface of GO through ATRP was accomplished in this study, and subsequently applied it to cement-based composites. The results indicate that the modified graphene oxide (GO) shows the decreased presence of surface hydroxyl groups. Furthermore, the electrostatic repulsion induced by the quaternised grafted polymer ensures the stability of QP4VP@GO in the cement hydration environment, effectively preventing the clustering of GO in the cement mortar. With a QP4VP@GO concentration of 0.03 wt. %,

the flexural strength of the cement composite at 28 days reaches its peak value of 8.0 MPa, marking a 42.3 % increase compared to conventional Portland cement and an 11.1 % improvement over cement samples with 0.03 wt. % GO. Similarly, at a QP4VP@GO concentration of 0.05 wt. %, the compressive strength at 28 days peaks at 72.4 MPa, showcasing a 63.1 % enhancement over Portland cement and a 16.6 % boost over cement samples doped with only 0.05 wt. % GO. QP4VP@GO contributes to improved cement hydration, hinders crack propagation, and enhances the mechanical characteristics of the cement composites. This study is expected to encourage the utilisation of GO in cement--based materials.

Acknowledgments

The authors kindly acknowledge the financial support from Heilongjiang University of Technology (No. 220704023).

REFERENCES

1. Sanchez F., Sobolev K. (2010): Nanotechnology in concrete-A review. *Construction and Building Materials, 24*, 2060-2071. doi: 10.1016/j.conbuildmat.2010.03.014
2. Basquiroto de Souza F., Yao X., Lin J., Naseem Z., Tang Q.Z., Hu Y., Gao W., Sagoe-Crentsil K., Duan W. (2022): Effective strategies to realize high-performance graphene-reinforced cement composites. *Construction and Building Materials, 32*4, 126636. doi: 10.1016/j.conbuildmat.2022.126636
3. Asim N., Badiei M., Samsudin N.A., Mohammad M., Razali H., Soltani S., Amin N. (2022): Application of graphene-based materials in developing sustainable infrastructure: An overview, *Composites Part B: Engineering, 245*, 110188. doi: 10.1016/j.compositesb.2022.110188
4. Xu Z., Huang Z., Liu C., Deng H., Deng X., Hui D., Zhang X., Bai Z. (2021): Research progress on key problems of nanomaterials-modified geopolymer concrete. *Nanotechnology Review, 10*, 779-792. doi: 10.1515/ntrev-2021-0056
5. Xu Z., Huang Z., Liu C., Deng X., Hui D., Deng Y., Zhao M., Qin L. (2021): Experimental study on mechanical properties and microstructures of steel fiber-reinforced fly ash-metakaolin geopolymer-recycled concrete. *Reviews on Advanced Materials Science, 60*, 578-590. doi: 10.1515/rams-2021-0050
6. Cao M., Xu L., Zhang C. (2018): Rheological and mechanical properties of hybrid fiber reinforced cement mortar. *Construction and Building Materials, 171*, 736-742. doi: 10.1016/j.conbuildmat.2017.09.054
7. Liu C., Huang X., Wu Y.Y., Deng X., Liu J., Zheng Z., Hui D. (2020): Review on the research progress of cement-based and geopolymer materials modified by graphene and graphene oxide, *Nanotechnology Review, 9*, 155-169. doi: 10.1515/ntrev-2020-0014
8. Sheikh T.M., Anwar M.P., Muthoosamy K., Jaganathan J., Chan A., Mohamed A.A. (2021): The mechanics of carbon-based nanomaterials as cement reinforcement-A critical review, *Construction and Building Materials, 303*, 124441. doi: 10.1016/j.conbuildmat.2021.124441
9. Zhang P., Wang M., Han X., Zheng Y. (2023): A review on properties of cement-based composites doped with graphene. *Journal of Building Engineering, 70*, 106367. doi: 10.1016/j.jobe.2023.106367
10. Zeng H., Qu S., Tian Y., Hu Y., Li Y. (2023): Recent progress on graphene oxide for next-generation concrete: Characterizations, applications and challenges. *Journal of Building Engineering, 69*, 106192. doi: 10.1016/j.jobe.2023.106192
11. Wang Q., Qi G.d., Wang Y., Zheng H.Y., Shan S.h., Lu C.X. (2021): Research progress on the effect of graphene oxide on the properties of cement-based composites. *New Carbon Materials, 36,* 729-750. doi: 10.1016/s1872-5805(21)60071-9
12. Liu C., Chen F., Wu Y., Zheng Z., Yang J., Yang B., Yang J., Hui D., Luo Y. (2021): Research progress on individual effect of graphene oxide in cement-based materials and its synergistic effect with other nanomaterials. *Nanotechnology Review, 10*, 1208-1235. doi: 10.1515/ntrev-2021-0080
13. Balaji S., Swathika A. (2022): Review on mechanical and microstructural properties of cementitious composites with graphene oxide. *Materials Today: Proceedings, 50*, 2280-2287. doi: 10.1016/j.matpr.2021.09.544
14. Yang S., Jia W., Wang Y., Zhang W., Yuan X. (2021): Hydroxylated graphene: A promising reinforcing nanofiller for nanoengineered cement composites. *ACS Omega, 6,* 30465-30477. doi: 10.1021/acsomega.1c03844
15. Muthu M., Yang E.H., Unluer C. (2021): Resistance of graphene oxide-modified cement pastes to hydrochloric acid attack. *Construction and Building Matering, 273,* 121990. doi: 10.1016/j.conbuildmat.2020.121990
16. Li X., Wang L., Liu Y., Li W., Dong B., Duan W.H. (2018): Dispersion of graphene oxide agglomerates in cement paste and its effects on electrical resistivity and flexural strength. *Cement & Concrete Composites, 92*, 145-154. doi: 10.1016/j.cemconcomp.2018.06.008
17. Park S., Lee K.S., Bozoklu G., Cai W., Nguyen S.T., Ruoff R.S. (2008): Graphene oxide papers modified by divalent ions-enhancing mechanical properties via chemical cross-linking. *ACS Nano, 2*, 572-578. doi: 10.1021/nn700349a
18. Li X., Korayem A.H., Li C., Liu Y., He H., Sanjayan J.G., Duan W.H. (2016): Incorporation of graphene oxide and silica fume into cement paste: A study of dispersion and compressive strength. *Construciton and Building Materials, 123*, 327-335. doi: 10.1016/j.conbuildmat.2016.07.022
19. Zhao L., Guo X., Liu Y., Ge C., Chen Z., Guo L., Shu X., Liu J. (2018): Investigation of dispersion behavior of GO modified by different water reducing agents in cement pore solution. *Carbon, 127*, 255-269. doi: 10.1016/j.carbon.2017.11.016
20. Nguyen H.D., Zhang Q., Sagoe-Crentsil K., Duan W. (2021): Graphene oxide-coated sand for improving performance of cement composites. *Cement and Concrete Composites, 124*, 104279. doi: 10.1016/j.cemconcomp.2021.104279
21. Rahmani S., Sharif A., Habibnejad Korayem A. (2021): Dispersion stability of chitosan grafted graphene oxide nanosheets in cementitious environments and their effects on the fluidity of cement mortar nanocomposites. *Journal of Appllied Polymer Science, 139*, 52095. doi: 10.1002/app.52095

22. Zhang X., Du M., Fang H., Shi M., Zhang C., Wang F. (2021): Polymer-modified cement mortars: Their enhanced properties, applications, prospects, and challenges. *Construction and Building Materials, 299*, 124290. doi: 10.1016/j.conbuildmat.2021.124290
23. Zhang X., Su Y., Lei L., Wu S., Shen J. (2021): Preparation of a three-dimensional modified graphene oxide via RAFT polymerization for reinforcing cement composites. *Colloids Surface Physicochemical Engeering Aspects, 610*, 125925. doi: 10.1016/j.colsurfa.2020.125925
24. Liu B., Wang L., Pan G., Li D. (2022): Dispersion of graphene oxide modified polycarboxylate superplasticizer in cement alkali solution for improving cement composites. *Journal of Building Engeering, 57*, 104860. doi: 10.1016/j.jobe.2022.104860
25. Xia J., Zhang X., Matyjaszewski K. (1999): Atom transfer radical polymerization of 4-vinylpyridine. *Macromolecules, 32*, 3531-3533. doi: 10.1021/ma9816968
26. Liu F., Eisenberg A. (2003): Synthesis of poly(tert-butyl acrylate)-block-polystyrene-block-poly(4-vinylpyridine) by living anionic polymerization. *Angewandte Chemie International Edition, 42*, 1404-1407. doi: 10.1002/anie.200390361
27. Vidts K.R.M., Du Prez F.E. (2006): Design of water-soluble block copolymers containing poly(4-vinylpyridine) by atom transfer radical polymerization. *European Polymer Journal, 42*, 43-50. doi: 10.1016/j.eurpolymj.2005.10.013
28. Lv S., Ma Y., Qiu C., Sun T., Liu J., Zhou Q. (2013): Effect of graphene oxide nanosheets of microstructure and mechanical properties of cement composites. *Construction and Building Materials, 49*, 121-127. doi: 10.1016/j.conbuildmat.2013.08.022
29. Li W., Li X., Chen S.J., Liu Y.M., Duan W.H., Shah S.P. (2017): Effects of graphene oxide on early-age hydration and electrical resistivity of Portland cement paste. *Construction and Building Materials, 136*, 506-514. doi: 10.1016/j.conbuildmat.2017.01.066
30. Bai S., Jiang L., Xu N., Jin M., Jiang S. (2018): Enhancement of mechanical and electrical properties of graphene/cement composite due to improved dispersion of graphene by addition of silica fume. *Construction and Building Materials, 164*, 433-441. doi: 10.1016/j.conbuildmat.2017.12.176
31. Li X., Liu Y.M., Li W.G., Li C.Y., Sanjayan J.G., Duan W.H., Li Z. (2017): Effects of graphene oxide agglomerates on workability, hydration, microstructure and compressive strength of cement paste. *Construction and Building Materials, 145*, 402-410. doi: 10.1016/j.conbuildmat.2017.04.058
32. Long W.J., Wei J.J., Xing F., Khayat K.H. (2018): Enhanced dynamic mechanical properties of cement paste modified with graphene oxide nanosheets and its reinforcing mechanism. *Cement & Concrete Composites, 93*, 127-139. doi: 10.1016/j.conbuildmat.2017.12.176
33. X. Yan, D. Zheng, H. Yang, H. Cui, M. Monasterio, Y. Lo, (2020): Study of optimizing graphene oxide dispersion and properties of the resulting cement mortars. *Construction and Building Materials, 257*, 345-354. doi: 10.1016/j.conbuildmat.2020.119477
34. Liu H., Yu Y., Liu H., Jin J., Liu S. (2018): Hybrid effects of nano-silica and graphene oxide on mechanical properties and hydration products of oil well cement. *Construction and Building Materials, 191*, 311-319. doi: 10.1016/j.conbuildmat.2018.10.029
35. Hou D., Yang T., Tang J., Li S. (2018): Reactive force-field molecular dynamics study on graphene oxide reinforced cement composite: functional group de-protonation, interfacial bonding and strengthening mechanism. *Physics Chemistry Chemistry Physics, 20*, 8773-8789. doi: 10.1039/c8cp00006a
36. Fu Q., Wang Z., Xue Y., Niu D. (2023): Catalysis and regulation of graphene oxide on hydration properties and microstructure of cement-Based materials. *ACS Sustainable Chemistry & Engineering, 11*, 5626-5643. doi: 10.1021/acssuschemeng.3c00109
37. Yao X., Shamsaei E., Sagoe-Crentsil K., Duan W. (2022): The interaction of graphene oxide with cement mortar: implications on reinforcing mechanisms. *Journal of Materials Science, 57*, 3405-3415. doi: 10.1007/s10853-021-06808-y.